The dimer interface of the SARS coronavirus nucleocapsid protein adapts a porcine respiratory and reproductive syndrome virus-like structure

Chung-ke Chang[a,1], Shih-Che Sue[a,1], Tsan-hung Yu[a], Chiu-Min Hsieh[a], Cheng-Kun Tsai[a,c], Yen-Chieh Chiang[a], Shin-jye Lee[a], Hsin-hao Hsiao[a], Wen-Jin Wu[a], Chi-Fon Chang[b], Tai-huang Huang[a,b,c,*]

[a] *Institute of Biomedical Sciences, Academia Sinica, Nankang, Taipei, Taiwan, ROC*
[b] *Genomic Research Center, Academia Sinica, Nankang, Taipei, Taiwan, ROC*
[c] *Department of Physics, National Taiwan Normal University, Taipei, Taiwan, ROC*

Received 31 August 2005; accepted 13 September 2005

Available online 30 September 2005

Edited by Miguel De la Rosa

Abstract We have employed NMR to investigate the structure of SARS coronavirus nucleocapsid protein dimer. We found that the secondary structure of the dimerization domain consists of five α helices and a β-hairpin. The dimer interface consists of a continuous four-stranded β-sheet superposed by two long α helices, reminiscent of that found in the nucleocapsid protein of porcine respiratory and reproductive syndrome virus. Extensive hydrogen bond formation between the two hairpins and hydrophobic interactions between the β-sheet and the α helices render the interface highly stable. Sequence alignment suggests that other coronavirus may share the same structural topology.

Keywords: SARS; Coronavirus; Capsid protein; NMR; Oligomerization

1. Introduction

Severe acute respiratory syndrome (SARS) is the first emerging infectious disease in the 21st century with a fatality rate of ca. 8% and is caused by a novel coronavirus (CoV) [1]. The nucleocapsid protein is a key component of the virus and is essential for virus formation. It binds to the viral RNA to form a ribonucleoprotein core, which can enter the host cell and interact with cellular processes [2–5]. The free protein presumably exists as a dimer in solution, with the dimerization domain located at the C-terminus [6,7]. We have previously defined the structural domains of the SARS-CoV N protein [8]. The C-terminal structural domain coincides with the dimerization domain identified in previous studies, and our biochemical studies showed that it exists as a dimer in solution. Denaturation studies have shown that dissociation of the SARS-CoV N protein is coupled with loss of structure, implying a structure-dependent mechanism for self-association [9]. Understanding this mechanism would not only provide insights into the viral assembly process, but also identify additional targets for drugs to combat SARS through disruption of N protein self-association. However, there has been no 3D structure of the dimerization domain of coronavirus N protein published and the underlining principle governing the self-association of coronavirus N protein dimer is also unknown. We have employed nuclear magnetic resonance (NMR) techniques to investigate the structure of the dimerization domain of SARS-CoV N protein. We report our results in this communication.

2. Materials and methods

2.1. Plasmid construction

SARS-CoV TW1 strain cDNA clones were kindly provided to us by Dr. P.-J. Chen of National Taiwan University Hospital [10]. The a SARS-CoV nucleocapsid protein fragment consisting of residues 281–365 ($NP_{281–365}$) and a SARS-CoV nucleocapsid protein fragment consisting of residues 248–365 ($NP_{248–365}$) clones were obtained by polymerase chain reaction (PCR) on a RoboCycler Gradient 96 (Stratagene, CA, USA) using appropriate primers. The resulting PCR fragment contained an *Nco*I site at one end and a *Bam*HI site at the other. After restriction enzyme digestion, the resulting fragment was cloned into the pET6H plasmid, which contains a His-tag coding region. The resultant protein fragment included an extra MHHHHHHAMG sequence at the N-terminus.

2.2. Protein expression and purification

The fragments corresponding to residues 248–365 ($NP_{248–365}$) and 281–365 ($NP_{281–365}$) of SARS-CoV N proteins were expressed in *Escherichia coli* BL21(DE3) strain. Isotopically labeled protein samples were prepared by culturing the cells in standard M9 media, supplemented with $^{15}NH_4Cl$ (1 g/L) (For ^{15}N-labeling) and/or u-^{13}C-glucose (2 g/L) (For ^{13}C-labeling) and appropriately labeled Isogro (0.5 g/L) (Isotec, OH, USA). Perdeuterated isotopically labeled protein samples were prepared by culturing the cells in the same media in D_2O (80% D_2O for samples used in filtered experiments) and supplemented with deuterated Isogro and glucose. Deuteration rates for all clones were on the order of 85% (65% for samples used in filtered experiments) as measured by mass spectrometry. The cells were broken with a microfluidizer and the protein purified through a Ni-NTA affinity column (Qiagen, CA, USA) in buffer (50 mM sodium phosphate, 150 mM NaCl, and pH 7.4) containing 7 M urea. The protein was then allowed to refold by dialysis in liquid chromatography buffer (50 mM sodium phosphate, 150 mM NaCl, 1 mM EDTA, 0.01% NaN_3, and pH 7.4).

*Corresponding author. Fax: +886 2 2788 7641.
E-mail address: bmthh@gate.sinica.edu.tw (T.-h. Huang).

[1] These authors contributed equally to this project.

Abbreviations: $NP_{248–365}$, a SARS-CoV nucleocapsid protein fragment consisting of residues 248–365; $NP_{281–365}$, a SARS-CoV nucleocapsid protein fragment consisting of residues 281–365; PRRSV, porcine reproductive and respiratory syndrome virus

0014-5793/$30.00 © 2005 Published by Elsevier B.V. on behalf of the Federation of European Biochemical Societies.
doi:10.1016/j.febslet.2005.09.038

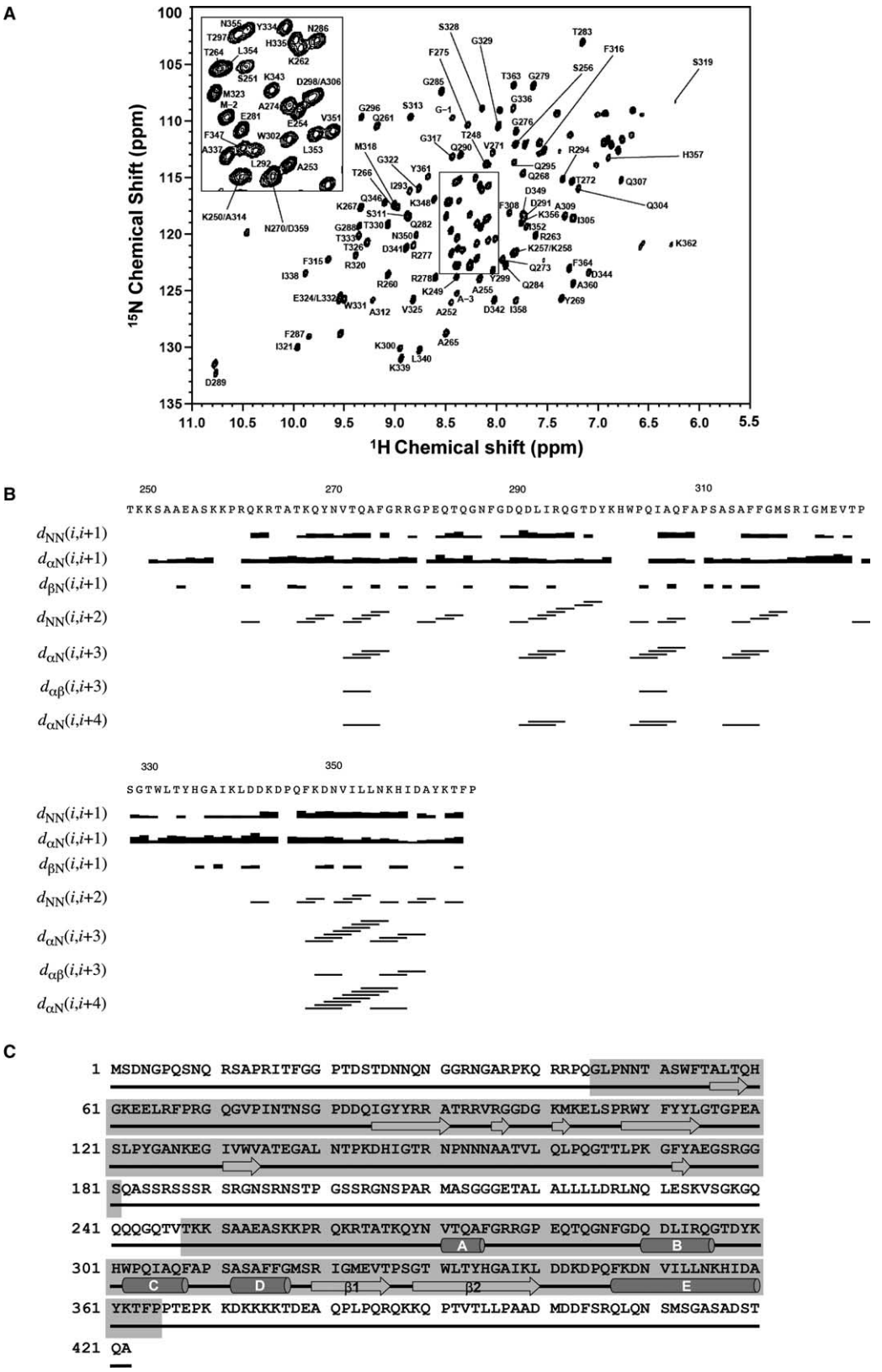

Fig. 1. (A) ^{15}N-HSQC spectrum of u-^{15}N-NP$_{248–365}$. (B) Summary of the NMR parameters employed for secondary structure prediction. Dots at the top indicate residues' NH protons are protected from deuterium exchange after 24 h. (C) Secondary structure profile of the SARS-CoV N protein. The two shaded areas represent the N-terminal and C-terminal structural domains. Secondary structure of the N-terminal domain was adapted from Huang et al. [27].

Renatured protein was loaded onto an AKTA-EXPLORER fast performance liquid chromatography (FPLC) system equipped with a Hi-Load 16/60 Superdex 75 column (Amersham Pharmacia Biotech, Sweden). Complete Protease Inhibitor cocktail (Roche, Germany) was added to the purified protein. Protein concentration was determined with the Bio-Rad Protein Assay kit as per instructions from the manufacturer (Bio-Rad, CA, USA). The correct molecular weight of the expressed protein was then confirmed by mass spectroscopy.

2.3. NMR spectroscopy

Protein samples for NMR experiments contain between 0.5 and 3 mM protein in NMR buffer (10 mM sodium phosphate buffer, pH 6.0, containing 50 mM NaCl, 1 mM EDTA, 1 mM 2,2-dimethyl-2-silapentane-5-sulfonate (DSS), 0.01% NaN_3, 10% D_2O and complete protease inhibitor cocktail). All NMR data were acquired at 30 °C on 500, 600 or 800 MHz Bruker AVANCE spectrometers equipped with a triple resonance TXI cryoprobe with an actively-shielded Z-gradient. Experimental parameters were set as described previously [11,12]. Sequential backbone resonance assignments for $^1H^N$, ^{15}N, $^{13}C_\alpha$ and $^{13}C_\beta$ were derived from standard 3D HNCA, HN(CO)CA, HNCO, HN(CA)CO, CBCANH, and CBCA(CO)NH experiments [13]. $(H_m)C_mCH$-TOCSY experiments were also obtained to correct for isotope effect on ^{13}C chemical shifts [14]. The assignments of H_α and H_β resonances were achieved from analysis of the HBHA(CO)NH spectrum. H(CC)(CO)NH, CC(CO)NH and HCCH-TOCSY spectra were analyzed to obtain side chain assignments. To identify the interface region involved in dimer interactions, $F_1[^{13}C, ^{15}N]$-filtered, F_3-^{15}N-edited and $F_1[^{13}C, ^{15}N]$-filtered, F_3-^{13}C-edited 3D NOESY-HSQC spectra were obtained using a (u-^2H,^{13}C,^{15}N)$NP_{248–365}$(65% deuteration)/$NP_{248–365}$ hetero-dimer sample prepared by mixing labeled $NP_{248–365}$ sample with equal amount of unlabeled $NP_{248–365}$ sample [15,16]. The protein was denatured in 8 M urea and renatured by extensive dialysis in desired NMR buffer conditions. Data were processed with the XWINNMR suite and AURELIA software (Bruker, Germany) on SGI workstations or NMRPipe on Linux workstations [17]. The ^1H chemical shift was referenced to DSS at 0 ppm as suggested [18].

2.4. Static light scattering

Protein samples in NMR buffer were diluted to a concentration between 0.5 and 2 mg/ml. Prior to loading into the cuvette, samples were filtered through a 0.22 μm-cutoff filter. Data were acquired on a DynaPro MS/X light scattering system equipped with a fixed-angle detector (Protein Solutions, NJ, USA) at 4 °C. Analysis was carried out on the

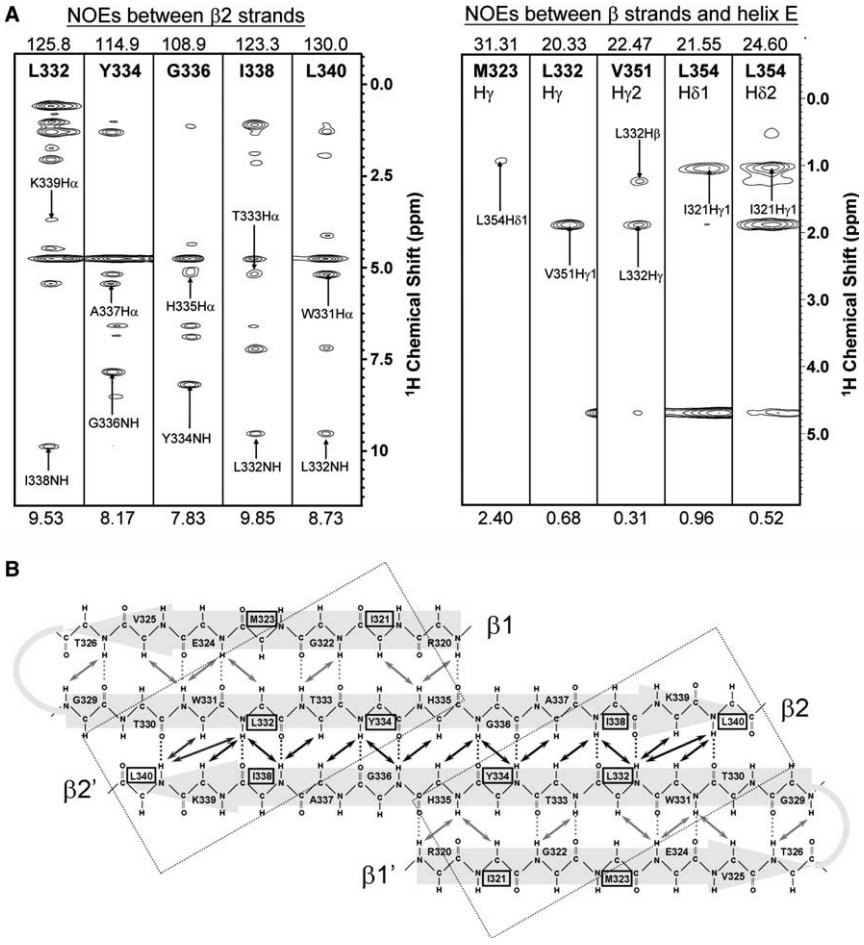

Fig. 2. (A) Stripe plots showing the intermolecular NOE connectivities in the β-sheet (left panel) and between the side chain resonances of residues in the β_2 strand of one monomer (labeled on top of the stripes) and side chain resonances of residues in E helix in the other monomer (indicated by arrows) (right panel). The stripes on the left panel were selected from the $F_1[^{13}C, ^{15}N]$-filtered, F_3-^{15}N-edited 3D NOESY-HSQC spectrum and the stripes on the the right panel were selected from the $F_1[^{13}C, ^{15}N]$-filtered, F_3-^{13}C-edited 3D NOESY-HSQC. (B) NOE connectivities of the β-sheet forming the dimer interface. The shaded arrows and the connecting loops represent the two β hairpins of the two monomers. The two-headed arrows show the observed NOE pairs and the dotted lines are the proposed hydrogen bonds stabilizing the β hairpins, as well as the dimer interface between the two β hairpins. The dotted rectangular boxes represent the positions of the two helices which interact with the four-stranded β-sheet. The boxed residues are those involved in hydrophobic interaction with the helices. The NOEs between β1 and β2 (also β1′ and β2′ in the other monomer) were obtained from 3D ^{15}N-NOESY-HSQC spectrum of u-^{15}N-$NP_{248–365}$ sample and the interfacial NOEs between β2 and β2′ were obtained from ^{15}N-filtered 3D NOESY-HSQC spectrum of sample containing u-(^2H, ^{13}C, ^{15}N)-$NP_{248–365}$(65% Deuteration)/unlabeled $NP_{248–365}$ hetero-dimer.

Dynamics V6 program suite included in the system on an IBM PC-compatible computer. Concentration effects were corrected within the program.

2.5. Chemical cross-linking

The homobifunctional amine cross-linker disuccinimidyl suberate was purchased from Sigma–Aldrich (MO, USA) and prepared in *N*,*N*-dimethylformamide (DMF) to a concentration of 25 mg/ml. Reactions were carried out with a final protein concentration of 0.35 mM and final cross-linker concentration of 5 mM. Mock reactions were set up as control which contained only the protein solution and DMF without cross-linker. The reaction mixtures in NMR buffer were allowed to react for 1 h at 4 °C prior to quenching with 100 mM glycine. The results were visualized on SDS-PhastGel minigels (Pharmacia Biotech, Sweden).

3. Results and discussion

3.1. Secondary structure of the dimerization domain

We have previously shown that SARS-CoV N protein consists of two structured domains, the RNA binding domain (a.a. 45–181) and the dimerization domain (a.a. 248–365), with the remainders of the sequence existing in disordered state [8]. $NP_{248–365}$ is the most stable domain which retains the dimer structure. Shortening the fragment causes structural changes and lengthening the fragment has no effect on the structure of $NP_{248–365}$. Backbone assignment for most amino acids of $NP_{248–365}$ was achieved except for residues located at the N-terminus and H301 (Fig. 1A). Perdeuteration of $NP_{248–365}$ was necessary to obtain triple-resonance spectra due to short T_2 (transverse relaxation time) of the dimer. The secondary structure of $NP_{248–365}$ was determined from standard NMR parameters, such as the characteristic NOE patterns, the consensus chemical shift indices (CSI), the magnitude of the $^3J_{HN\alpha}$ value, and the H^N exchange rates (Fig. 1B). The result shows that $NP_{248–365}$ consists of five α-helices (A, Val271-Phe274; B, Gln290-Gln295; C, Trp302-Phe308; D, Ala312-Gly317 and E, Phe347-Ala360) and two β strands (β1: Arg320-Thr326; β2: Gly329-Leu340) (see Fig. 1C).

3.2. The dimer interface is composed of a β-sheet stabilized by helix E

The short T_2 of the $NP_{248–365}$dimer (MW = 28 kD) precluded full assignment of side chain resonances due to weak signals even on cryoprobe-equipped spectrometers, thus hampered complete 3D structure determination of the dimer to high resolution. However, most H_α, H_β and aliphatic side-chain nuclei could be assigned from $(H_m)C_mCH$-TOCSY, HCCH-TOCSY and ^{13}C-edited NOESY spectra. Further analysis of the intramolecular dimer-interface NOEs identified a number of contacts between the two β strands, which allowed us to define the β hairpin structure (Fig. 2A). This information allowed us to manually assign the intermolecular NOEs at the dimer interface from analysis of the $F_1[^{13}C, ^{15}N]$-filtered, F_3-^{15}N-edited and $F_1[^{13}C, ^{15}N]$-filtered, F_3-^{13}C-edited 3D NOESY-HSQC spectra using u-(^2H,^{13}C,^{15}N)$NP_{248–365}$(65% deuteration)/unlabeled-$NP_{248–365}$ sample. Our results indicate that the dimer interface is composed of a continuous four-stranded β-sheet, formed by extensive hydrogen bond interactions between the two long β strands of the two β-hairpins, contributed one from each of the two monomers (Figs. 2B and 3A). The dimer is further stabilized by hydrophobic interactions between residues on one side of the amphipathic long helix E and the β-sheet (Fig. 3B). The presence of the extensive interactions between the two monomers in a dimer provides strong stabilization force and explains why the two monomers cannot be separated without denaturing the protein, even though there is no cysteine in the dimerization domain to form a covalent disulfide bond. This arrangement is reminiscent of

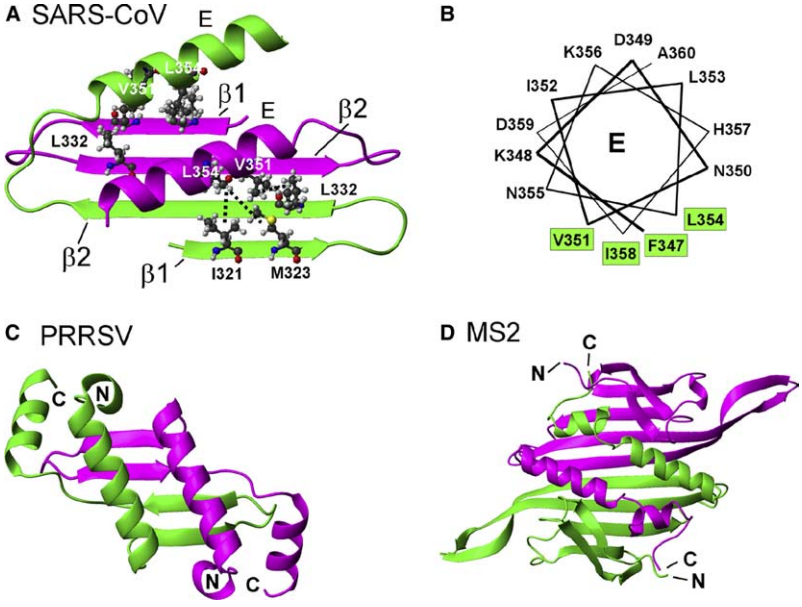

Fig. 3. (A) Schematic representation of the structure of the dimer interface of SARS-CoV N protein. The relative orientation between the anti-parallel β-sheet and the E helix is defined by the six NOEs identified as shown on Fig. 2A. Residues involved in these NOEs are shown in stick and ball representations. (B) Helical wheel plot of helix E, showing the amphipathic nature of the helix. The hydrophobic face is defined by the four hydrophobic residues (colored green). (C) Ribbon representation of the structure of the dimer interface of the C-terminal domain of the nucleocapsid protein of porcine reproductive and respiratory syndrome virus (PRRSV) (PDB ID: 1P65). (D) Ribbon representation of the structure of the dimer interface of the capsid protein of bacteriophage MS2 (PDB ID: 1AQ3). The ribbon representations are prepared with the MOLMOL program.

the dimer-interface of the porcine reproductive and respiratory syndrome virus (PRRSV) nucleocapsid protein (Fig. 3C) [19], the coat protein of bacteriophage MS2 (Fig. 3D) [19] and the peptide recognition domain of the human histocompatibility antigen (HLA) [20,21].

3.3. The stable dimer interface is an ideal common building block for dimer interfaces

It has been postulated that although coronaviruses are evolutionary related to arteriviruses, the large size discrepancy of their nucleocapsid proteins most likely implied that they had different folds [22]. However, we show that there are common principles that underlie the architecture of a nucleocapsid protein in both SARS-CoV and PRRSV. They both contain two regions, one for RNA-binding and the other for dimerization or oligomerization [8,23], albeit the two domains in SARS-CoV N protein is linked by a much longer flexible linker of ~120 a.a. Most importantly, the structures of the dimer interface of the two viruses are very similar. The presence of extensive interactions in the dimer interface may render this

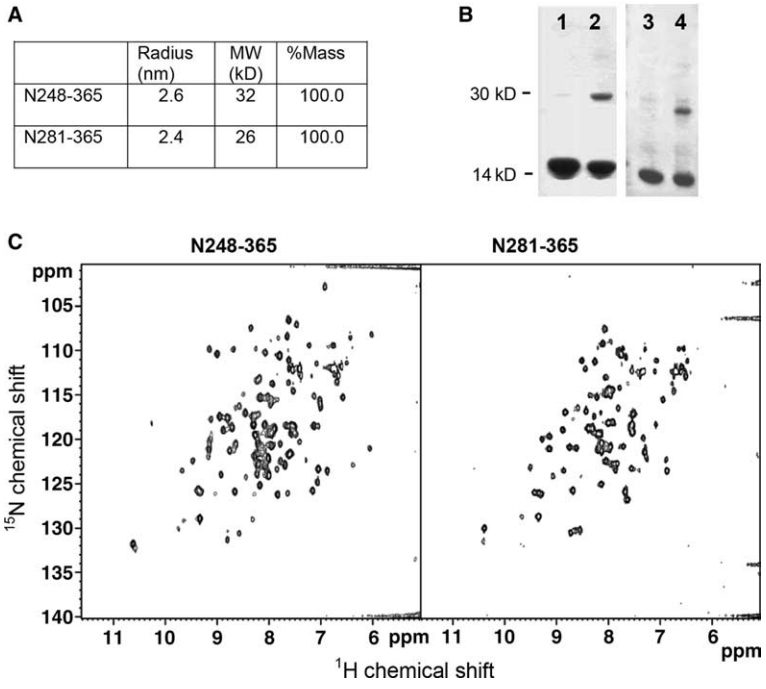

Fig. 4. (A) Light scattering results of $NP_{248–365}$ and $NP_{281–365}$. Estimated particle radii and molecular weights are listed. (B) Chemical cross-linking of $NP_{248–365}$ (lanes 1 and 2) and $NP_{281–365}$ (lanes 3 and 4). Lanes 1 and 3: without cross-linker. Lanes 2 and 4: with cross-linker. (C) ^{15}N-edited HSQC spectra of $NP_{248–365}$ (left) and $NP_{281–365}$ (right).

```
SARS CoV      319 SRIGMEVTP-----------SGTWLTYHGAIKLDDKDPQFKDNVILLNKHID 358
                  -EEEEE---***********--EEEEEEEEEEE--------HHHHHHHHH--
TGEV          291 SYWTSKEDG-----------DQIEVTFTHKYHLPKDDPKTEQFLQQINAYAR 331
                  --EE-----***********--EEEEEEEEEEE--------HHHHHH-----
FCoV          287 SQWSAEEAG-----------DQVKVTLTHNYYLPKDDAKTSQFLEQIDAYKR 327
                  -EEEE----***********--EEEEEE-EEE------HHHHHHHHHHH---
HCoV 229E     306 SHIVSKESG-----------NTVVLTFTTRVTVPKDHPHLGKFLEELNAFTR 346
                  -EEEE----***********--EEEEEEEEEEE------HHHHHHHHHHH--
BCoV          327 SRLELAKVQNLSGNLDEPQKDVYELRYNGAIRFDSTLSGFETIMKVLNENLN 378
                  -HHHHHHHH-------------EEEEE---EE--------HHHHHHHHHHHH
HCoV OC43     327 SRLELAKVQNLSGNPDEPQKDVYELRYNGAIRFDSTLSGFETIMKVLNENLN 378
                  -HHHHHHH--------------EEEEE---EE--------HHHHHHHHHHHH
PHEV          327 SRLELAKVQNLSGNPDEPQKDVYELRYNGAIRFDSTLSGFETIMKVLNQNLN 378
                  --HHHHHH--------------EEEEE---EE--------HHHHHHHHHHHH
MHV-1         328 SKLELVKKN--SGGADDPTKDVYELQYSGAIRFDSTLPGFETIMKVLNENLD 377
                  -EEEE----**---------EEEEEEE--EEE---------HHHHHHHHHH-
IBV           285 SRVTPKLQP-----------DGLHLKFEFTTVVPRDDPQFDNYVKICDQCVD 325
                  -EEE-E---***********--EEEEEEEEEEE-------HHHHHHHHHH--
```

Fig. 5. Alignment of the amino acid sequences of various coronavirus N proteins. The alignment shows only the regions corresponding to the dimer interface region of SARS-CoV. From top to bottom: SARS-CoV, porcine transmissible gastroenteritis virus (TGEV), feline coronavirus (FCoV), human coronavirus strain 229E (HCoV 229E), bovine coronavirus (BCoV), human coronavirus strain OC43 (HCoV OC43), porcine hemagglutinating encephalomyelitis virus (PHEV), murine hepatitis virus 1 (MHV-1) and avian infectious bronchitis virus (IBV). JPred secondary structure predictions of the sequences are shown below the sequences. E and H represent the predicted secondary structure of a particular amino acid as β-strand or α helix, respectively.

dimer interface to become self-contained, i.e., it is less likely to be dependent on the global structure of the protein. In fact, we have found that a.a. $NP_{281–365}$ still retained dimerization potential, even though structural differences were evident from NMR spectra (Fig. 4). Similar observations have been reported in the literature [6]. It is evident that the tight dimer interface structure permits certain extended perturbation in the global structure without affecting the dimer structure. Such characteristics make this particular fold ideal as a common building block for dimer interfaces in a variety of proteins.

3.4. The dimerization mechanism may be common among coronavirus nucleocapsid proteins

To investigate whether all coronavirus N proteins share this dimerization mechanism we have used ClustalX to align the sequences of other coronaviruses [24] and the resulting subsequences were then submitted to the JPred server for secondary structure prediction [25]. Sequence alignment coupled with secondary structure prediction show that many share the ββα topology observed in SARS-CoV (Fig. 5). In particular, the long β-strand and the long C-terminal helix are predicted to be present in all cases. Most of them also contain the short β-strand, with the exceptions of BCoV, HCoV and PHEV. These results raise the possibility that all coronavirus employ the same interface mechanism for dimerization and they belong to the same structural class, however this cannot be verified by the class-dependent prediction algorithm because of the lack of known tertiary structure [26].

In conclusion, we have determined the secondary structure of the dimerization domain of SARS-CoV N protein and have mapped out the residues involved in the interface. We show that the interface of SARS-CoV N protein dimer is a four-stranded β-sheet, superposed by two long helices. The topology closely resembles that of the PRRSV nucleocapsid protein and the coat protein of bacteriophage MS2. This type of dimer interfaces is highly stable and could serve as one of the common building blocks for dimer interfaces in nature. Sequence alignment and secondary structure prediction suggest that other coronavirus N proteins also adopt a similar dimerization mechanism.

Acknowledgments: This work was supported in part by the Academia Sinica and by grants (Grants NSC 92-2113-M-001-056 and NSC 92-2751-B-001-020-Y) from the National Science Council of the Republic of China. The NMR spectra were obtained at the High-field Nuclear Magnetic Resonance Center (HF-NMRC), National Research Program for Genomic Medicine (NRPGM), Taiwan, ROC.

References

[1] Lai, M.M. (2003) SARS virus: the beginning of the unraveling of a new coronavirus. J. Biomed. Sci. 10, 664–675.
[2] Ng, M.L., Tan, S.H., See, E.E., Ooi, E.E. and Ling, A.E. (2003) Early events of SARS coronavirus infection in vero cells. J. Med. Virol. 71, 323–331.
[3] Surjit, M., Liu, B., Jameel, S., Chow, V.T. and Lal, S.K. (2004) The SARS coronavirus nucleocapsid protein induces actin reorganization and apoptosis in COS-1 cells in the absence of growth factors. Biochem. J. 383, 13–18.
[4] Luo, H., Chen, Q., Chen, J., Chen, K., Shen, X. and Jiang, H. (2005) The nucleocapsid protein of SARS coronavirus has a high binding affinity to the human cellular heterogeneous nuclear ribonucleoprotein A1. FEBS Lett. 579, 2623–2628.
[5] He, R. et al. (2003) Activation of AP-1 signal transduction pathway by SARS coronavirus nucleocapsid protein,. Biochem. Biophys. Res. Commun. 311, 870–876.
[6] Yu, I.M., Gustafson, C.L., Diao, J., Burgner 2nd, J.W., Li, Z., Zhang, J. and Chen, J. (2005) Recombinant severe acute respiratory syndrome (SARS) coronavirus nucleocapsid protein forms a dimer through its C-terminal domain. J. Biol. Chem. 280, 23280–23286.
[7] Surjit, M., Liu, B., Kumar, P., Chow, V.T. and Lal, S.K. (2004) The nucleocapsid protein of the SARS coronavirus is capable of self-association through a C-terminal 209 amino acid interaction domain. Biochem. Biophys. Res. Commun. 317, 1030–1036.
[8] Chang, C.-k. et al. (in press) Modular organization of SARS coronavirus nucleocapsid protein. J. Biomed. Sci.
[9] Luo, H. et al. (2004) In vitro biochemical and thermodynamic characterization of nucleocapsid protein of SARS. Biophys. Chem. 112, 15–25.
[10] Yeh, S.-H. et al. (2004) Characterization of severe acute respiratory syndrome coronavirus genomes in Taiwan: Molecular epidemiology and genome evolution. PNAS 101, 2542–2547.
[11] Sue, S.C., Chang, J.Y., Lee, S.C., Wu, W.G. and Huang, T.-h. (2004) Solution structure and heparin binding site of hepatoma-derived growth factors. J. Mol. Biol. 343, 1365–1377.
[12] Lin, T.H., Chen, C.P., Huang, R.F., Lee, Y.L., Shaw, J.F. and Huang, T.H. (1998) Multinuclear NMR resonance assignments and the secondary structure of Escherichia coli thioesterase/protease I: A member of a new subclass of lipolytic enzymes. J. Biomol. NMR 11, 363–380.
[13] Bax, A. and Grzesiek, S. (1993) Methodological advances in Protein NMR. Acc. Chem. Res. 26, 131–138.
[14] Yang, D., Zheng, Y., Liu, D. and Wyss, D.F. (2004) Sequence-specific assignments of methyl groups in high-molecular weight proteins. J. Am. Chem. Soc. 126, 3710–3711.
[15] Zwahlen, C., Legault, P., Vincent, S.J.F., Greenblatt, J., Konrat, R. and Kay, L.E. (1997) Methods for measurement of intermolecular NOEs by multinuclear NMR spectroscopy: application to a bacteriophage N-peptide/boxB RNA complex. J. Am. Chem. Soc. 119, 6711–6721.
[16] Iwahara, J., Wojciak, J.M. and Clubb, R.T. (2001) Improved NMR spectra of a protein–DNA complex through rational mutagenesis and the application of a sensitivity optimized isotope-filtered NOESY experiment. J. Biomol. NMR 19, 231–241.
[17] Delaglio, F., Grzesiek, S., Vuister, G.W., Zhu, G., Pfeifer, J. and Bax, A. (1995) NMRPipe: a multidimensional spectral processing system based on UNIX pipes. J. Biomol. NMR 6, 277–293.
[18] Wishart, D.S., Bigam, C.G., Yao, J., Abildgaard, F., Dyson, H.J., Oldfield, E., Markley, J.L. and Sykes, B.D. (1995) 1H, 13C, 15N chemical shift referencing in biomolecular NMR. J. Biomol. NMR 6, 135–140.
[19] Cahill, D.P., Lengauer, C., Yu, J., Riggins, G.J., Wilson, J.K., Markowitz, S.D., Kinzler, K.W. and Vogelstein, B. (1998) Mutations of mitotic checkpoint genes in human cancers. Nature 392, 300.
[20] Valegard, K., Lijas, L., Fridborg, K. and Unge, T. (1990) The three dimensional structure of the bacterial virus MS2. Nature 345, 36–41.
[21] Sape, M.A., Bjorkman, P.J. and Wiley, D.C. (1991) Refined structure of the human histocompatibility antigen HLA-A2 at 2.6A resolution. J. Mol. Biol. 219, 277–319.
[22] Strauss, E., Strauss, J. (2002) Viruses and Human Diseases, Academic Press, San Diego, CA, USA.
[23] Doan, D.N. and Dokland, T. (2003) Structure of the nucleocapsid protein of porcine reproductive and respiratory syndrome virus. Structure (Camb) 11, 1445–1451.
[24] Thompson, J., Gibson, T., Plewniak, F., Jeanmougin, F. and Higgins, D. (1997) The CLUSTAL_X windows interface: flexible strategies for multiple sequence alignment aided by quality analysis tools. Nucl. Acids Res. 25, 4876–4882.
[25] Cuff, J., Clamp, M., Siddiqui, A., Finlay, M. and Barton, G. (1998) JPred: a consensus secondary structure prediction server. Bioinformatics 14, 892–893.
[26] Cohen, B.I., Presnell, S.R. and Cohen, F.E. (1993) Origins of structural diversity within sequentially identical hexapeptides. Protein Sci. 2, 2134–2145.
[27] Huang, Q. et al. (2004) Structure of the N-terminal RNA-binding domain of the SARS CoV nucleocapsid protein. Biochemistry 43, 6059–6063.